Observing Southern California Landslides Using UAVSAR: La Conchita as a Case Study

Nathan Pulver[1], Andrea Donnellan[2], Jay Parker[3], and Lindsay LaBrecque[4]

[1]Jet Propulsion Laboratory
[2]Jet Propulsion Laboratory, California Institute of Technology & University of Southern California
[3]Jet Propulsion Lab (NASA)
[4]Stanford University

November 22, 2022

Abstract

The La Conchita Landslide is infamous for its repeated devastation of the coastal community in Southern California. The landslide caused severe damage and loss of life once in 1995 and 2005. In this study we use UAVSAR interferograms of the La Conchita area to identify any residual motion or slope instability associated with the landslides. UAVSAR is NASA's airborne interferometric synthetic aperture radar (InSAR) platform and is useful for imaging changes in the Earth's surface. UAVSAR repeat pass interferometry products show disturbances in the image pairs that may correlate with landslides, including where the La Conchita landslides had previously occurred. We used UAVSAR to compare different line-of-sight velocity profiles of the landslide to a stable area to the northeast. UAVSAR pairs show ongoing motion of up to -0.14 cm/day average velocity years after the landslides occurred. More stable areas show less than -0.06 cm/day maximum average velocity. The results imply that damaged rock and soil of a landslide continue to move relative to the surrounding more stable area. UAVSAR image pairs may be useful for identifying unstable areas on slopes that may be associated with landslides or other disturbances.

Observing Southern California Landslides Using UAVSAR: La Conchita as a Case Study

Nathan Pulver[1,2], Andrea Donnellan[1], Jay Parker[1], Lindsay LaBrecque[3,1]

1. Jet Propulsion Laboratory, California Institute of Technology
2. California State Polytechnic University, Pomona
3. Stanford University, Palo Alto

Abstract

The La Conchita Landslide is infamous for its repeated devastation of the coastal community in Southern California. The landslide caused severe damage and loss of life once in 1995 and 2005. In this study we use UAVSAR interferograms of the La Conchita area to identify any residual motion or slope instability associated with the landslides. UAVSAR is NASA's airborne interferometric synthetic aperture radar (InSAR) platform and is useful for imaging changes in the Earth's surface. UAVSAR repeat pass interferometry products show disturbances in the image pairs that may correlate with landslides, including where the La Conchita landslides had previously occurred. We used UAVSAR to compare different line-of-sight velocity profiles of the landslide to a stable area to the northeast. UAVSAR pairs show ongoing motion of up to -0.14 cm/day average velocity years after the landslides occurred. More stable areas show less than -0.06 cm/day maximum average velocity. The results imply that damaged rock and soil of a landslide continue to move relative to the surrounding more stable area. UAVSAR image pairs may be useful for identifying unstable areas on slopes that may be associated with landslides or other disturbances.

Main Points

1. UAVSAR repeat pass interferometry products show disturbances in the image pairs that may correlate with landslides.
2. UAVSAR observations over the 1995 and 2005 La Conchita landslides show continued disturbance.
3. UAVSAR image pairs may be useful for identifying landslide areas where damaged rock and soil continue to move.

Background

Tectonic deformation, subsidence, erosion, deposition, debris flows, and landslides all modify the Earth's surface. UAVSAR, NASA's airborne interferometric synthetic aperture radar (InSAR) platform, images the Earth's surface and change. The UAVSAR project has been collecting repeat pass interferometry (RPI) over southern California since 2009, primarily to study tectonic motions and earthquakes. During this time, however, a variety of land surface processes have been observed, including landslides. For this paper we focus on the La Conchita landslide area which had its last large mass movement in 2005, yet shows surface motions in UAVSAR image pairs all of which have timeframes several years after the most recent landslide. This large, well-documented landslide provides an excellent case study for comparison with UAVSAR.

La Conchita

La Conchita is a coastal community in southern California, located southeast of Santa Barbara and northwest of Ventura. The cliffs surrounding the community are made up of marine sediments, which are poorly indurated shale sandstone and conglomerates of the Pico and Saugus formations (Putnam, 1942). The Punta Gorda terrace, in the middle of the La Conchita community, rises 1300 feet above sea level and was estimated to be at sea level between 35,000 and 60,000 years ago (Harden, 1986). This young terrace is well known to have frequent mass movements, with records dating back to the 1800s (Hemphill, 2001). Putnam (1942) noted that nearly the entire area underlain by upper Pico Shale is currently in motion downslope, or has moved very recently. The La Conchita community was initially developed in 1924. The most recent major landslides were in 1995 and 2005.

In 1995, the area surrounding La Conchita received an abnormally high amount of rainfall. The annual mean rainfall from October through March is 390 mm in the area. 1994-1995 had about 761mm of rainfall in the same time frame, with about 21mm occurring in moderate storm days before the slide. As a result, the earth above the community moved at 2:03PM PST on March 4, 1995. The slide moved tens of meters in minutes, leaving 9 houses destroyed or damaged. Six days later, a debris flow from the canyon damaged another 5 houses in the northwest part of the community. The slide was 120m wide by 330m long and its base was estimated to be at a depth greater than 30m giving a volume of approximately 1.3×10^6 m^3 (Jibson, 2005).

The 2005 mass movement occurred on January 10^{th}. The majority of the slide consisted of the southeast portion of the 1995 landslide; nearly all of the material was also part of the 1995 slide. This slide was only about 15% of the volume of the 1995 slide, at 200,000 m^3. Although the more recent slide was significantly smaller in volume, it destroyed and damaged many more structures and caused loss of life. 13 houses were destroyed, 23 were severely damaged, and 10 confirmed deaths occurred. Leading up to the slide, record amounts of rainfall fell in the area. At a station 20 km southeast of La Conchita, rainfall from October 2004 to January 2005 was up by roughly 400% compared to the annual mean in the same months. This was not from one extreme storm. Consistent rainfall for the 15 days prior to the slide proved lethal to the integrity of the slope.

UAVSAR Interferometry

UAVSAR collects L-band radar images in swaths about 20 km wide and up to 200 km long looking left from the airborne instrument at an oblique range of elevation angles of 27 to 63°. The L-band radar instrument is fully polarimetric and housed in a pod that is mounted on the underside of a Gulfstream-III aircraft. Precision autopilot is used when collecting radar data which allows the aircraft to repeat a path within a 5 m radius tube; that is, the aircraft repeats the pass within a few meters at a later time. Two images collected at different times are processed to produce an image of change between the two passes by comparing the phases of the radar returns. The resulting image is a map of line-of-sight phase differences, which can be mapped to displacements. In cases where the ground is too disrupted it is not possible to compare phase and the image decorrelates, leaving data gaps, in those regions. Data gaps can also occur for steep terrain where mountainous areas can block or shadow the radar signal from the surface. UAVSAR measurements have a ground pixel size of about 1 m for raw RPI products and 7 m for unwrapped products in which the phase change is converted, or unwrapped, to displacement values (Donnellan et al, 2014).

Though UAVSAR observations were collected for measuring crustal deformation, other surface displacements and disruption can be observed in the radar imagery. For example, both the Thomas Fire and ensuing Montecito debris flows were identified in UAVSAR data products (Donnellan et al, 2018). UAVSAR unwrapped interferograms were used to develop a three-dimensional flow model for the Slumgullion slow landslide in Colorado (Delbridge et al, 2016). In analyzing the UAVSAR RPI images across the greater Los Angeles area we observe numerous features that appear to be landslides. Southern California landslides have particular characteristics that differ from landslides in Northern California and elsewhere (Scott McCoy, written communication) and understanding the regional characteristics of landslides is important for forecasting them. The presence of roots modifies the shear resistance of hillslopes (Schmidt et al, 2001). Wildfires, earthquakes, debris flows, and landslides can all disrupt root systems, making the land surface susceptible to new or additional sliding. Disruption of root systems, particularly in steep terrain can exacerbate landslide susceptibility (Montgomery et al, 2000). Topography, weather, tectonics, human activity and geological structure influence typical regional landslide features, such as the rugged slopes of the Transverse and Coastal ranges, the sloping deposits of clay soil subject to frequent rainfall in the Berkley Hills, and the rapidly uplifted sedimentary breccia, deep canyons and wet climate of the heavily logged Eel river region.

We focus on southern California UAVSAR measurements to analyze the potential value of identifying landslides with UAVSAR data and to better understand how landslides are observed with UAVSAR in southern California. We start with the well understood La Conchita landslides and observations of UAVSAR RPI products collected 2010 – 2014 that show InSAR phase deviations coincident with the location of the landslides. This serves as a starting point to understand the utility of UAVSAR for studying landslides and for possibility relating whether observed landslides are the result of wildfires, earthquakes, other disruption of root systems, or storms.

Methods

We use UAVSAR image pairs for this study because there is a copious amount of data covering many different time frames in the period 2010 – 2014. Landslides can have a fairly small scale and UAVSAR has the advantage of higher resolution data compared to satellite-based InSAR. The UAVSAR pixel resolution of ~1 m for raw products and ~7 m for unwrapped products (Donnellan et al, 2018) is about 10x better than ~100 m resolution for spaceborne L-band InSAR data. The UAVSAR project produces many products, but for the purposes of this paper, we work with the unwrapped interferograms, which are available for download at GeoGateway (Donnellan et al, 2021; http://geo-gateway.org). GeoGateway allows users to create profiles of ground range change for any UAVSAR interferogram, allows for preliminary data exploration of unwrapped interferograms, and provides download links for the available products of that interferogram. Ground range change is defined as the motion of a pixel on the ground toward (positive) or away (negative) from the aircraft.

We retrieved data via geo-gateway from the Alaska Satellite Facility, and explored and analyzed the data in ArcGIS Pro and Google Earth Pro. We plotted the landslide catalog from the California Geological Survey (CGS) in ArcGIS Pro in order to qualitatively assess the stability or landslide susceptibility of the region. For the interpretation of the UAVSAR data we also used Geo-gateway to create ground range change profiles of various interferograms or Repeat Pass Interferometry (RPI) products. The data were downloaded and plotted in Microsoft Excel. We searched for patterns and significant contrasts in color in the Interferograms. Ground range profiles helped identify distinct ground range change patterns and data gaps. Pixel based velocity measurements were calculated using the ground range profile data divided by the elapsed time for each interferogram. Possible noise in the interferograms was noted, and steps were taken to ensure we were not looking at a shadowed area, which is an area on the ground usually on a slope facing away from the instrument that is obscured by terrain.

We developed a python script, shadow2kml.py, to create a kml map of mountain-shadowed regions where radar line of sight lines are obscured, based on one UAVSAR repeat-pass interferogram (RPI). RPI images have been widely used to identify surface deformation in the time between passes, which is typically months to years for UAVSAR. The script processing requires local residence of two files downloaded from the remote archives, a text annotation file that corresponds to the RPI image, and a local digital elevation map (DEM). These two file types may be identified by their filenames, which are respectively of the form <tag>.ann and <tag>.hgt.grd, where <tag> is part of the filename provided by the organization that supplies the files. For example, one of our study interferograms has the <tag> SanAnd_08527_10072-007_10085-003_0054d_s01_L090HH_01. This <tag> includes the location of the observation, heading of the aircraft, identifiers of repeated flight lines, year and ordinal count within the year of the passes, and the days between passes. Details may be found at https://uavsar.jpl.nasa.gov/science/documents/rpi-format.html. The text annotation file contains metadata including an estimate of aircraft altitude and geometry and the rectilinear ground sample grid, which is a rectangular grid in longitude and latitude. The binary digital elevation map covers precisely the RPI map region, with the same sampling in coordinate space as the RPI image. Both file types are provided at the RPI specific page of the UAVSAR project, and freely distributed via the Alaska Satellite Facility. Discovery tools to identify UAVSAR flight lines, RPI pairs and related images are provided at geo-gateway.org and uavsar.jpl.nasa.gov. In the first phase of processing, the shadow2kml.py script computes a set of maps on a reduced set of pixels based on area-averaged original samples of the DEM. For each derived pixel on the ground these maps contain the estimated elevation angle to the radar instrument, the radar azimuth direction, and the ground topography gradient.

In the second phase, we consider a dense set of horizontal lines, one for each boundary pixel on the radar-near side of the image and extending in the azimuth direction. For each of these lines, the directional derivative of the elevation map (the component of slope along the azimuth direction) is compared with the local elevation angle of the radar, pixel by pixel. Where this slope matches the radar elevation, the ray grazes the surface, and pixels are marked in shadow from this pixel to points beyond. The far point of the shadow is determined by the next intersection of the ray from the grazing point with the landscape. This agrees with our experience of shadows: when walking away from the sun, descending a steep ridge into more moderate slopes, the sun is obscured by the ridge from the step where the sun's ray grazes the ridge, until at a more distant step the sun emerges above the ridge. This method necessarily neglects possible shadowing grazing points outside the of the RPI image and toward the radar, but such rare exceptions are usually easy to identify by consulting any topographic map of the broader region outside the provided DEM, which covers the RPI image only. Once the grazing points are identified and pixels on the ground-projected grazing lines that are away from the radar and lie below the grazing lines are identified for every slant line, those pixels determine a map of the obscured regions, which is the output as a Google Earth Keyhole Markup Language (kml) file. The obscured areas may be black or white depending on the option selected by the user, and all other pixels are rendered transparent so the kml image may simply be overlain with the RPI image or any other background in Google Maps or similar tools. In that way there is a simple visual distinction between areas of disordered ground returns due to obscuration and disordered returns due to local disturbances that reduce or eliminate radar coherence. This distinction is essential for distinguishing candidate areas where the RPI and RPI coherence have no relevant bearing on whether landslides are present or not and where the RPI data indicate good candidate areas for landslides for further study.

Results

We observe phase changes interpreted as surface motion in the UAVSAR products where the La Conchita landslides had occurred. This surface motion is apparent in the RPI images even though many years have passed since the last major mass movement. An outline of the movement indicated in the UAVSAR RPI product compares similarly to the more recent 2005 slide, with some crossover to the older sliding mass.

We observed differences in line of sight (LOS) velocities when viewing the landslide profiles for interferograms formed along UAVSAR flight line SanAnd_08527, shown in figures 6-9. This flight line observes the southwest-facing La Conchita slopes from the reasonably favorable south direction, from an elevation angle of about 27 degrees. Comparing the transection of the landslide (Fig. 6.) area and the stable test area to the east of it (Fig. 7), we see the velocities, computed from displacement and timespan, are initially very similar across nearly all of the interferograms. At approximately .09 km along the profile we see a gap in the data due to incoherence when viewing the transection of the Conchita landslide, making it difficult to draw any conclusions from this set. This incoherence aligns well with the 2005 sliding mass, indicating the 1995 sliding mass is currently relatively stable in comparison. When reviewing the head to toe profile of the 1995 and 2005 landslides, we see more jagged spikes in the velocity, with interferogram b showing a significant deviation from the rest in terms of velocity per pixel.

The shape of the sliding mass is consistent throughout the interferograms, indicating there is something causing displacements within the slide. According to the velocity plots, we see the slide is moving at a higher rate than the stable, flat area above. The average LOS velocities shown in Fig. 10 show a significant deviation from the stable area, particularly in the head-to-toe profiles. It is also important to note that the standard deviation of the velocities in the stable area is an order of magnitude lower than the standard deviations of the velocities in the head-to-toe 2005 profile. The standard deviation of the velocities in the stable area is .005 while the 2005 head-to-toe profile has a standard deviation of .012. Some of the interferograms (b, g, h in Fig. 5) seem to be less noisy, while still showing significant motion, while others have some range change in a seemingly random fashion.

Discussion

These observations suggest ongoing motion along the slope of the previous active landslides. The higher velocities and the incoherence both suggest some significant motion during recent times.

A higher standard deviation of the head-to-toe profile may indicate larger differences in motion but it is important to understand the geometry of the slope and the radar instrument. UAVSAR line 26 528 (interferograms c-h) is flown at an elevation angle of 46° above the horizon. The slope of the hillside varies, but ranges from 2 .35 ° in the first 200 meters from the south side of coast highway, 20.61° between 200-475 m from the highway, and 28.5 upslope elevation angle from 475-600 m. This means that the slope is not in the radar shadow, but the viewing angle is far from ideal and the return power of the radar signal may be reduced. The 08527 UAVSAR line (interferograms a,b) is flown at an elevation angle of 152° which is much more favorable for the viewing of the slope than line 26528. Downslope motion will be seen as opposite for these two UAVSAR lines. From the perspective of the 08527 line, downslope motion will be seen as moving towards the radar, with the opposite being true for the 26528 flight.

The Google Earth imagery in figure 11 shows that there are significant variations in vegetation growth depending on the season. There also seems to be a gully in the center of the 2005 sliding mass where water may collect, causing an increase in plant growth in that area. The motions we identify in the 2005 sliding mass could be due to changes in vegetation over the time between the two UAVSAR flights. It is also possible that the center area that seems to be consistently vegetated could be a spring that seeps out into the hillside. Rainfall data from the National Oceanic and Atmospheric Administration (NOAA) for the interferograms b and c show a small amount of rainfall over the time period. From July 2011 to October 2011, a weather station in Ventura, CA shows a total rainfall of 3 mm. October of 2010 to December of 2010 shows more significant amount of rainfall with approximately 280 mm. Rainfall could feed the hypothesized spring and cause a more active seep during and after heavy rainfall. The implications of this spring for the evolution of the landslide are important and further validation should be done.

Discerning the La Conchita slide is possible when we already know what the boundary of the slide looks like. The more challenging aspect is identifying landslides without direct field knowledge. The most obvious characteristic of landslides in these images is from the LOS data: the velocities in the head to toe profiles are more jagged, but still contain a clear trend in most of the interferograms. Noise exists in many forms in most RPI products, even with steps taken to reduce or remove it. Noise can be slight differences in flight path that were not completely accounted for, or atmospheric noise. Atmospheric noise and flight path variations are accounted for in the post-processing of the product, but there may be artifacts from unmodeled aircraft motion or atmospheric noise.

Future work should include stacking the data and carrying out time series analysis of the interferogram stack. Machine learning could also be applied to UAVSAR products in regions vulnerable to landslides to classify a feature in the data as a potential landslide. The main impedance would be finding or creating labeled data in this domain as there currently is no interferogram data with labeled features bound to an area of the image or data. Validation of the motion could be done through drone imaging, GPS monitoring, LIDAR scanning or other methods of change detection.

Conclusions

Using present-day UAVSAR observations we observed continued sliding in the areas of the 1995 and 2005 La Conchita landslides. UAVSAR pairs show continued sliding of up to -0.14 cm/day average velocity, while more stable areas show less than -0.06 cm/day maximum average velocity. The results show that years after major landslides the surface can continue to slip and that UAVSAR can detect the disturbance. The results imply that damaged rock and soil of a landslide continue to move relative to the surrounding more stable area. UAVSAR observations of this known landslide serve to demonstrate that UAVSAR can be a useful tool for identifying landslide prone regions. UAVSAR can be used in future studies to catalog past landslide activity in southern California and possibly whether they were triggered by earthquakes or resulted from denudation of vegetation from wildfires. Field studies using lidar (Light detection and ranging) scans or stereophotogrammetry from drone imagery could confirm the motion. More broadly, UAVSAR RPI products could be useful for the identification of smaller landslides or slope instabilities without prior field knowledge.

Acknowledgements

This work was carried out at the Jet Propulsion Laboratory, California Institute of Technology under contract with NASA. We thank the UAVSAR team for the data. Data can be accessed via the Alaska Satellite Facility or GeoGateway (http://geo-gateway.org).

References

Donnellan, A., Green, J., Ansar, A., Muellerschoen, R., Parker, J., Tanner, A., Lou, Y., Heflin, M., Arrowsmith, R., Rundle, J. and Ben-Zion, Y., 2018, July. Geodetic Imaging of Fault Systems from Airborne Platforms: UAVSAR and Structure from Motion. In *IGARSS 2018-* 2018 IEEE International Geoscience and Remote Sensing Symposium (pp. 7878-7881). IEEE.

Donnellan, A., Parker, J., Hensley, S., Pierce, M., Wang, J. and Rundle, J., 2014. UAVSAR Observations of Triggered Slip On the Imperial, Superstition Hills, and East Elmore Ranch Faults Associated with the 2010 M 7.2 El Mayor-Cucapah Earthquake. Geochemistry, Geophysics, Geosystems, 15(3), pp.815-829.

Donnellan, A., Parker, J., Milliner, C., Farr, T.G., Glasscoe, M., Lou, Y., Zheng, Y. and Hawkins, B., 2018. UAVSAR and Optical Analysis of the Thomas Fire Scar and Montecito Debris Flows: Case Study of Methods for Disaster Response Using Remote Sensing Products. Earth and Space Science, 5(7), pp.339-347.

Donnellan, A., Parker, J., Heflin, M., Glasscoe, M., Lyzenga, G., Pierce, M., Wang, J., Rundle, J., Ludwig, L.G., Granat, R. and Mirkhanian, M., 2021. Improving access to geodetic imaging crustal deformation data using GeoGateway. Earth Science Informatics, pp.1-13.

Harden, J.W., Sarna-Wojcicki, A.M. and Dembroff, G.R., 1986. Soils developed on coastal and fluvial terraces near Ventura, California (No. 1590-B). USGPO,.

Hemphill, J. (2001). Assessing Landslide Hazard over a 130-Year Period for La Conchita, California. [online] www.geog.ucsb.edu. Available at: http://www.geog.ucsb.edu/~jeff/projects/la_conchita/apcg2001_article/apcg2001_article.html [Accessed 27 Apr. 2020].

Jibson, R.W., 2005. Landslide hazards at La Conchita, California (p. 12). US Department of the Interior, US Geological Survey.

Putnam, W.C., 1942. Geomorphology of the Ventura region, California. Bulletin of the Geological Society of America, 53(5), pp.691-754.

Tables

Table 1. UAVSAR RPI products used and the associated dates flown and duration between the two passes.

Interferogram Information			
Tag	Dates Flown	Time Interval (days)	Figure Reference letter
SanAnd_08527_10072-007_10085-003_0054d_s01_L090HH_01	14-Oct-2010, 07-Dec-2010	54	b.
SanAnd_08527_11047-005_11068-004_0112d_s01_L090HH_01	8-Jul-2011, 28-Oct-2011	112	c.
SanAnd_26528_11047-006_12021-003_0294d_s01_L090HH_01	8-Jul-2011, 27-Apr-2012	294	d.
SanAnd_26528_12021-003_13096-005_0396d_s01_L090HH_01	27-Apr-2012, 28-May-2013	396	e.
SanAnd_26528_12135-007_13096-005_0190d_s01_L090HH_01	19-Nov-2012, 28-May-2013	190	f.
SanAnd_26528_13096-005_14006-005_0234d_s01_L090HH_01	28-May-2013, 17-Jan-2014	234	g.
SanAnd_26528_14006-005_14091-012_0158d_s01_L090HH_01	17-Jan-2014, 24-Jun-2014	158	h.

Figures

Figure 1. Overview map showing the location of La Conchita, along with other significant locations

Figure 2. La Chonchita area showing the 1995 slide in blue and the 2005 slide in yellow. The red is the outline of an inferred ancient landslide. Arrows indicate other minor slides in the area (Image from Jibson, 2005).

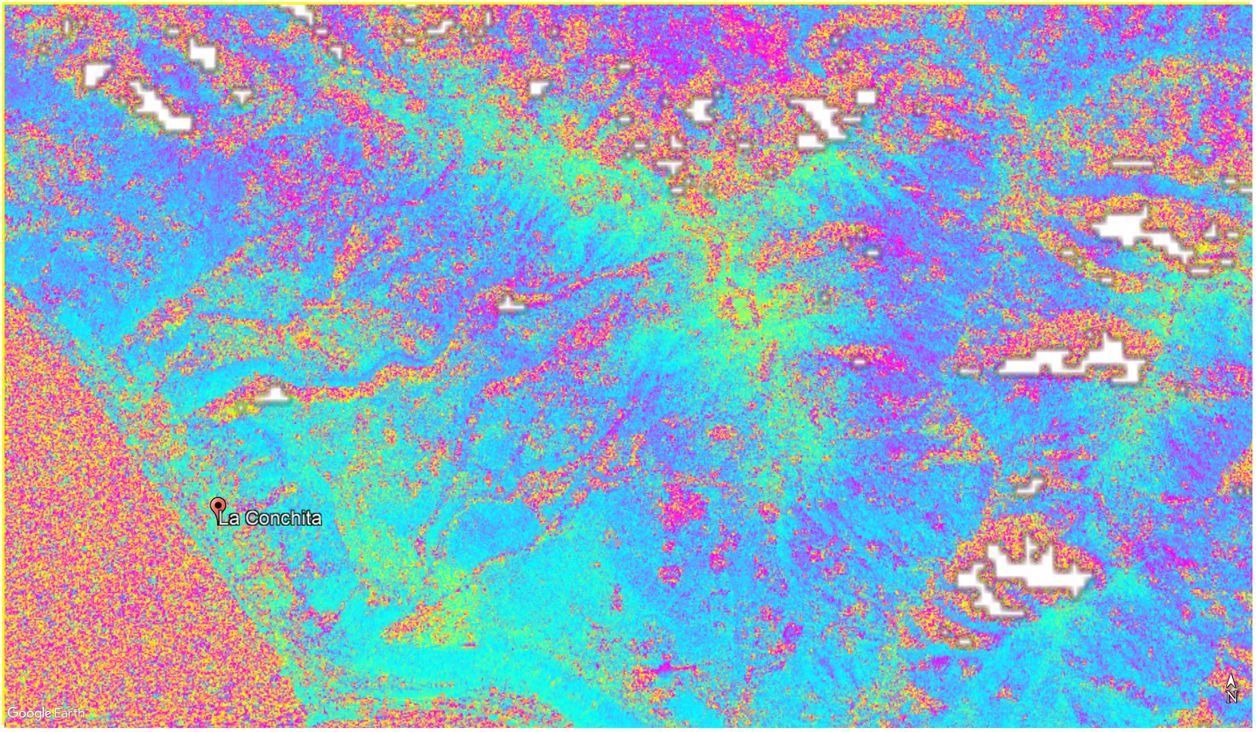

Figure 3. Example output of shadow2kml.py python script overlain onto an interferogram. Shadows are shown as white polygons. According to shadow2kml, La Conchita is not in a shadowed region.

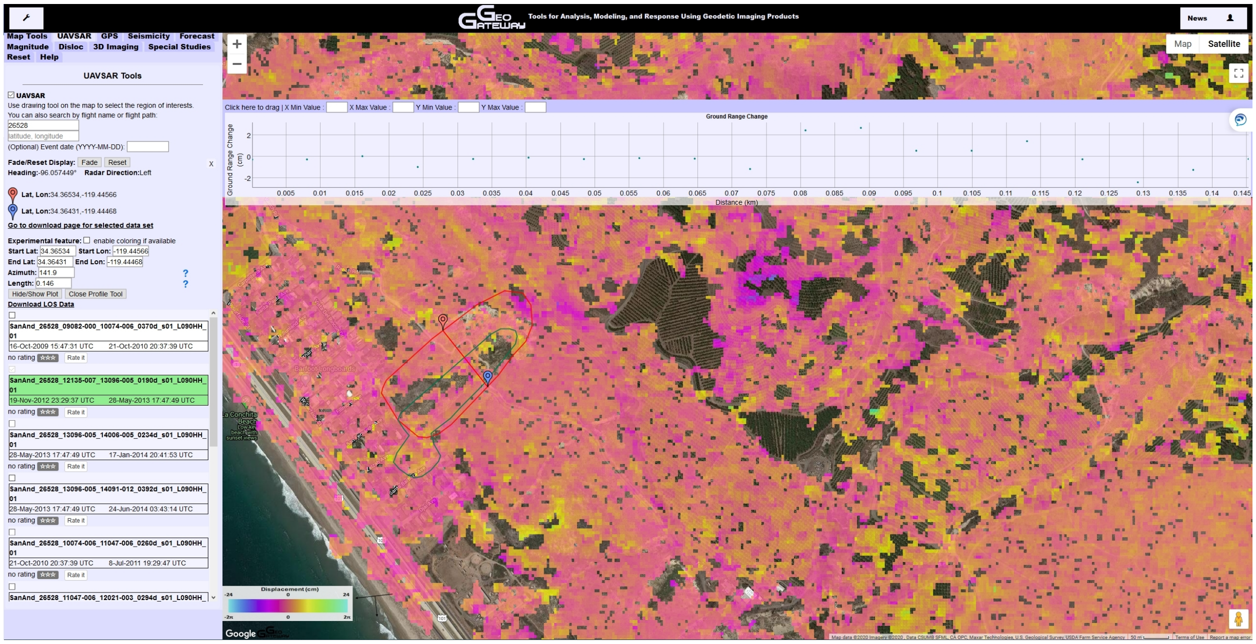

Figure 4. Example of geo-gateway.org interface. This image shows the use of the profile tool. The starting point is the red pin, and the ending point is the blue pin. These can be adjusted by hand or by entering coordinates and a length into the boxes on the left. You can also see the KML mapper tool being used. The La Conchita slides are outline in red (1995) and in green (2005). The interferogram shown is the unwrapped product, with the tag highlighted in green.

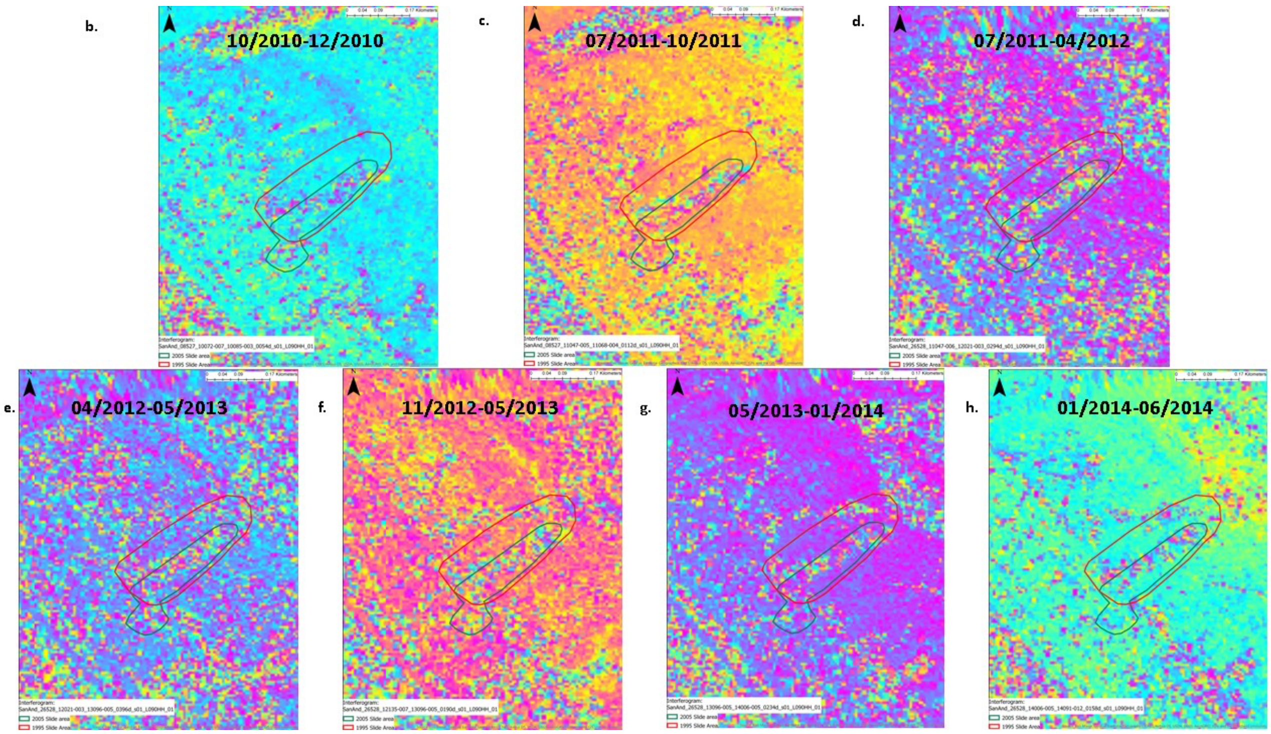

Figure 5. Panels b-h are interferograms covering the La Conchita community. The red outline indicates the 1995 slide and the green outline indicates the 2005 slide. Further descriptions of each interferogram can be found in Table 1.

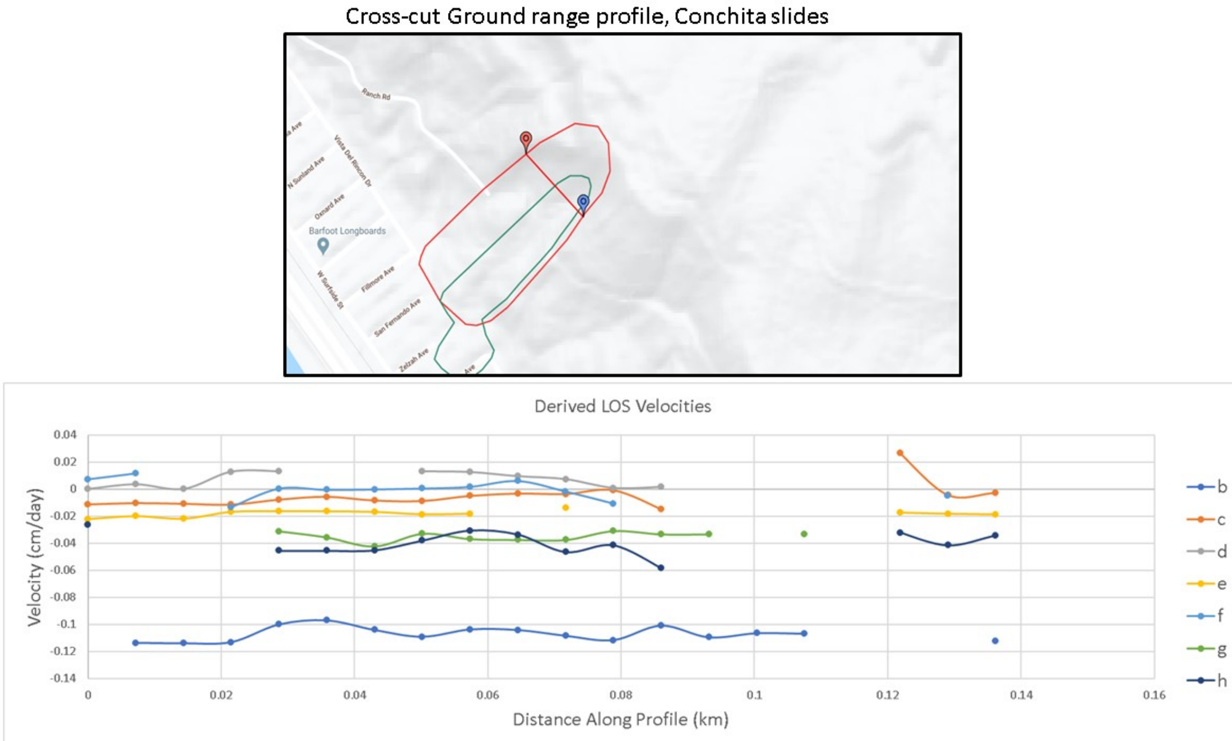

Figure 6. Ground range change profiles of each interferogram, starting on the red pin and ending on the blue pin. These profiles cross cut both of the slides, as shown in the upper left image. The profiles were created from the profile tool from geo-gateway.org. Note the scales for them are different, and each letter corresponds to the letter in table 1.

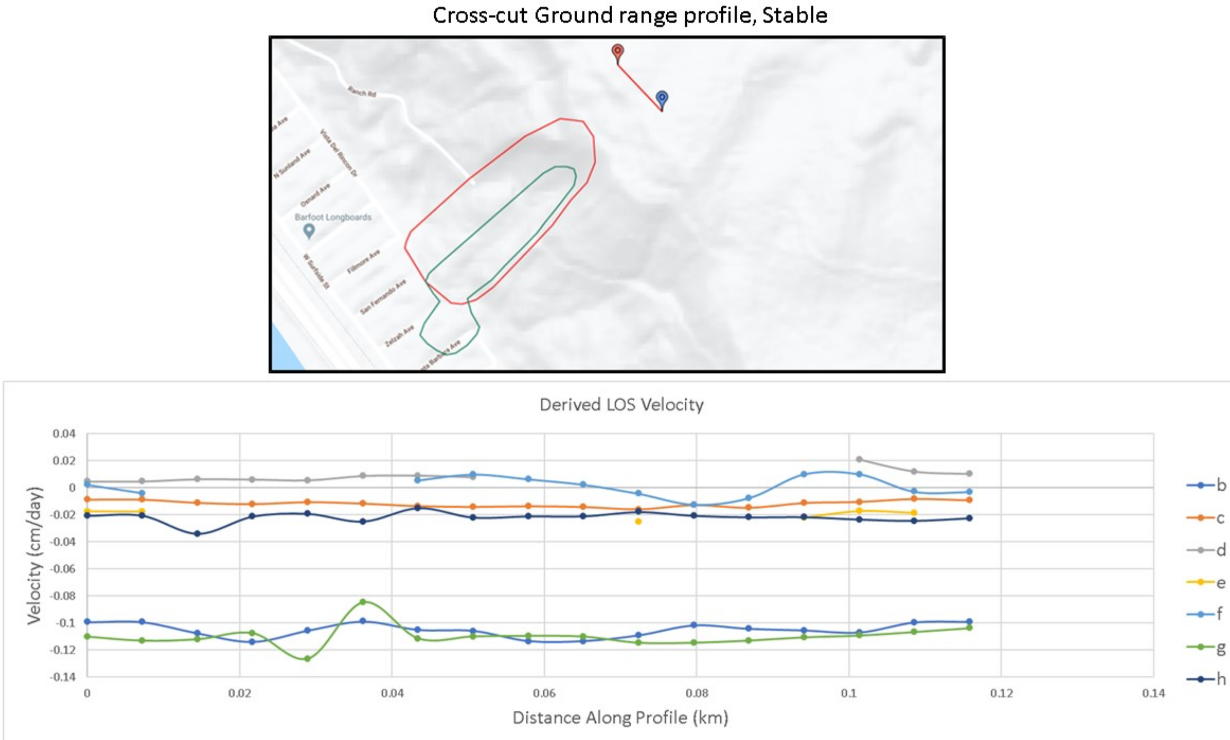

Figure 7. A control area to the north east of the slide. This area is agricultural land and has shown little change in the interferograms. It is made up of the same material as the sliding masses and this profile is similar to that in figure 5.

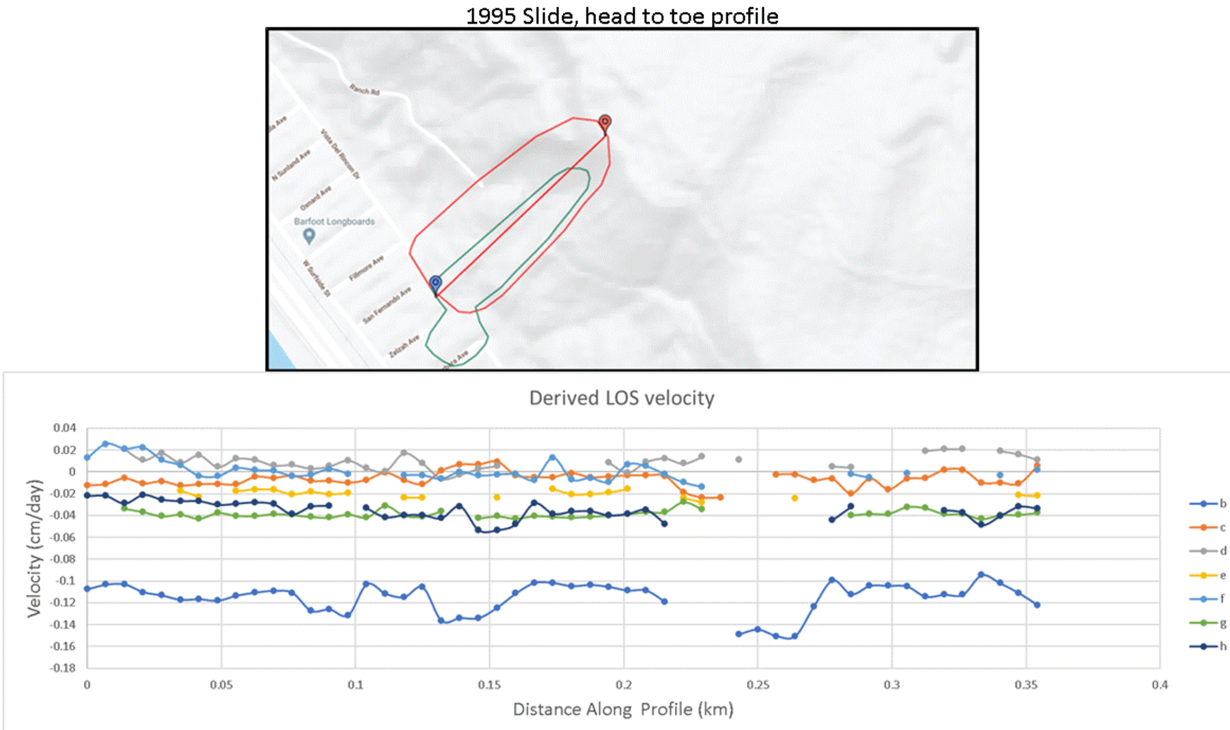

Figure 8. A head-to-toe profile of ground range change of the 1995 slide for each interferogram b-f. Letters b-h indicate the interferogram information as described in Table 1. Although this profile covers the 1995 slide area, it was intentionally taken to include the 2005 slide as well.

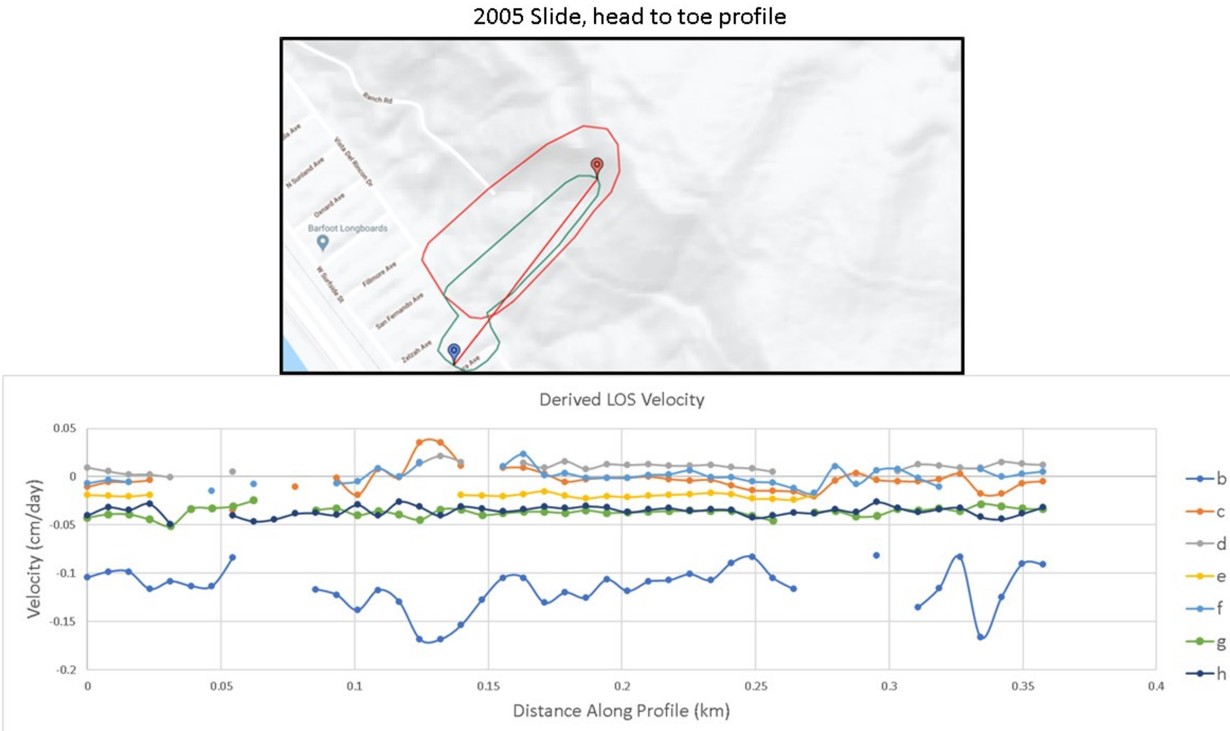

Figure 9. Ground range change profiles of interferograms b-h as referenced in Table 1. This profile mainly depicts change from the 2005 slide but also has crossover with the 1995 slide.

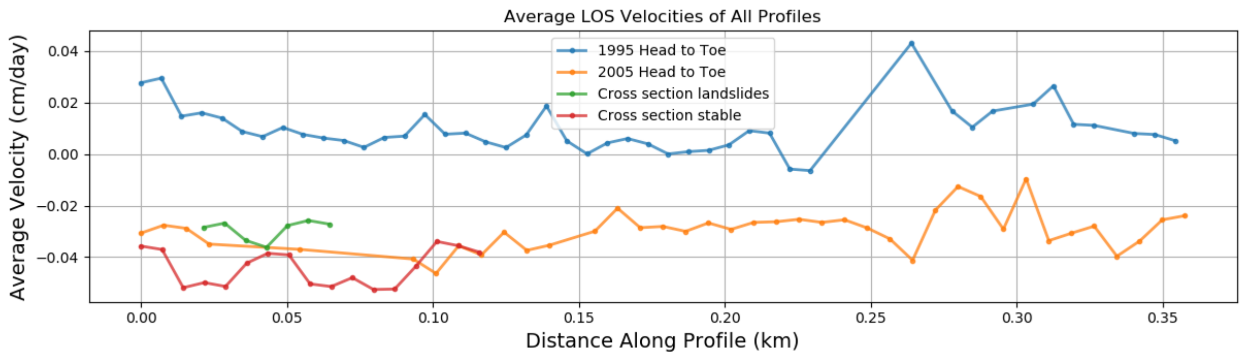

Figure 10. This plot shows the average pixel velocities for each profile shown in previous figures. Note, the length of each profile is not equivalent. In order to average all the interferograms with almost opposite look directions, the 08527 flights values were inverted. In order to remove any background displacements, the average RMS of the stable area was subtracted from all interferogram. A total of 7 interferograms were averaged for each profile. If an averaged data point had less than 5 values due to decorrelation in certain interferograms, the point was labeled an outlier and thrown out.

Figure 11. Google Earth Imagery from 2009 (left) and 2011 (right). Shows the variations in vegetation that could be responsible for some displacements seen in interferograms.